Assessment of Vascular Response after Stent Implantation by Intracoronary Optical Coherence Tomography

Yasushi Ino, Takashi Kubo*, Yoshiki Matsuo, Hironori Kitabata, Takeyoshi Kameyama, Atsushi Tanaka and Takashi Akasaka

Wakayama Medical University, 811-1 Kimiidera, Wakayama, Japan

Abstract: Optical coherence tomography (OCT) is a high resolution (10-20 μm) imaging modality that provides microscopic visualization of the coronary artery including vascular response after stent implantation. Compared to conventional intravascular ultrasound, OCT can more clearly identify findings immediately after stent implantation, such as tissue protrusion, stent edge dissection, and incomplete stent strut apposition. Furthermore, OCT allows clinicians to accurately assess the late acquired stent malapposition and strut coverage which could be a surrogate marker for stent thrombosis after drug-eluting stent (DES) implantation. OCT can evaluate not only the extent and amount of neointima but also the tissue characteristics of neointimal hyperplasia. Morphological OCT evaluation of restenosis tissue may offer important information about treatment strategies for in-stent restenosis lesion as well as the acute/mid-term clinical outcome after percutaneous coronary intervention. In addition, in-stent neoatherosclerosis, which are associated with very late stent failure, including stent thrombosis and restenosis, frequently has the following OCT findings; lipid-rich neointima, microvascular proliferation, and neointimal disruption. Thus, the high resolution imaging of OCT has provided important insights into the vascular response immediately and late after stent implantation.

Keywords: Optical coherence tomography, drug-eluting stent, vascular response, restenosis, neoatherosclerosis.

INTRODUCTION

Optical coherence tomography (OCT) is a catheter-based imaging system that uses near-infrared light to produce cross-sectional images of the coronary arteries. With its extraordinarily high resolution (10-20 μm), OCT allows clinicians to obtain detailed analysis of the coronary artery wall *in vivo*, including plaque characterization, identification of unstable plaque, and assessment of the vascular response immediately and late after stent implantation [1-5]. This review focuses on the usefulness of OCT in the assessment of vascular response after stent implantation.

CURRENT OCT TECHNOLOGY

The OCT system consists of a light source, reference mirror, and photodetector. Newer generations of intravascular OCT systems, termed frequency-domain (FD)-OCT, use a fixed mirror with a variable frequency light source, which allow fast image acquisition [3, 6-8]. At present, two OCT systems are clinically available; FD-OCT (St. Jude Medical, St. Paul, Minnesota, USA) and Optical Frequency Domain Imaging (OFDI) (Terumo, Tokyo, Japan) (Table **1**). The pullback speed of the OCT catheter is up to 20-40 mm/s, and the scanning length reaches 75-150 mm. In addition, FD-OCT imaging can be achieved during contrast injection from a guiding catheter (<15 ml, 3–4 ml/s). The high frame rate, fast pullback speed, and long pullback length of FD-OCT enable to image long coronary segments easily and safely [9-11].

ASSESSMENT IMMEDIATELY AFTER STENT IMPLANTATION

Tissue Protrusion

Tissue protrusion that includes plaque protrusion and thrombus protrusion is defined as the projection of tissue (> 50 μm) into the lumen between stent struts [3]. Plaque protrusion is characterized by a smooth surface structure without signal attenuation (Figure **1A**), whereas thrombus protrusion by an irregular surface with significant signal attenuation (Figure **1B**) [4, 12]. Tissue protrusion has been observed in the majority of lesions immediately after stent implantation (60-97.5%) [3,4,12,13]. The frequency of tissue protrusion detected by OCT was significantly higher than that of it detected by IVUS (18% - 35%) [3,4,12]. Tissue protrusion is frequently observed in the culprit lesion of acute coronary syndrome, because unstable lesion contains soft lipid tissue and thrombi (Figure **2**) [4]. The clinical significance of tissue protrusion is controversial. One pervious IVUS study has reported that the large tissue protrusion detected by IVUS was associated with early stent thrombosis after primary percutaneous coronary intervention (PCI) for ST-elevation myocardial infarction (STEMI) [14]. On the other hand, until now, no significant relationship between OCT-verified tissue protrusion and

*Address corresponding to this author at the Department of Cardiovascular Medicine, Wakayama Medical University, 811-1 Kimiidera, Wakayama, Japan; Tel: 81-73-447-2300; Fax: 81-73-446-0631;
E-mail: takakubo@wakayama-med.ac.jp

E-ISSN: 2311-052X/16

Table 1: Comparison of Frequency-Domain Optical Coherence Tomography (St. Jude Medical) and Optical Frequency Domain Imaging (Terumo)

	Frequency-domain optical coherence tomography (SJM, ILUMIEN OPTIS™)	**Optical Frequency Domain Imaging (TERUMO, LUNAWAVE™)**
Sheath priming (Closed/Open)	Required (Open)	Not required (Closed)
Length from tip to lens	27 mm	24 mm
Frame rate	180frame/sec	158frame/sec
Pullback speed	18/36mm/sec	Up to 40 mm/s (Customer- changeable)
Pullback length	54/75mm	Up to150 mm
Penetration depth	2 mm	no official data
Scan diameter	10mm	9 mm (in contrast) 10 mm (in saline)
Angio co-registration	Yes (only available for OPTIS Integrated System)	Yes
Dual review mode	No	Yes
3D reconstruction	Yes	Yes (with stent and guide wire emphasize)

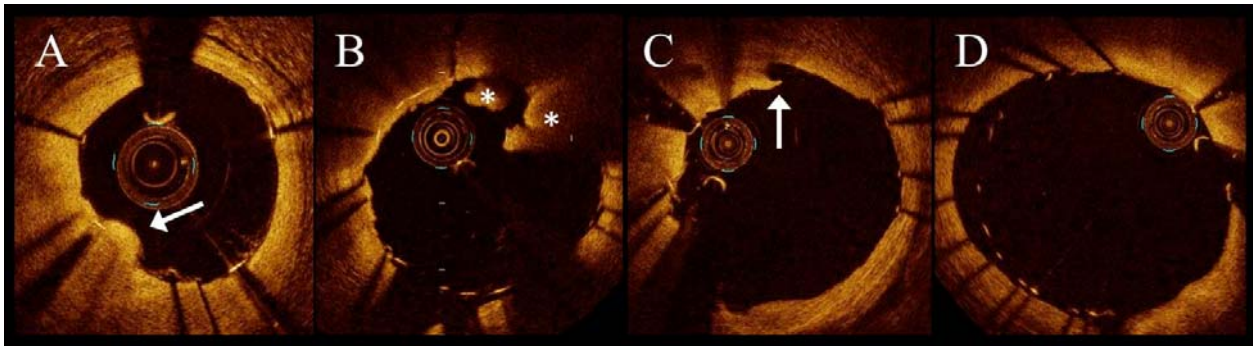

Figure 1: OCT findings immediately after stent implantation.

A; tissue protrusion (arrow), **B**; thrombus (dagger), **C**; edge dissection (arrow), **D**; incomplete stent strut apposition.

subsequent stent thrombosis/restenosis has been reported. Furthermore, previous studies using serial OCT examinations have reported that most tissue protrusions have resolved during 6-8 months follow-up [4,15,16].

Edge Dissection

OCT can also detect stent edge dissection better than IVUS (Figure **1C**) [3,4,12,15]. The incidence varies from 14 to 38 % and depends on plaque type at the stent edge; 35-38 % for fibrocalcific, 25-40 % for lipid-rich, and 9-30 % for fibrous plaque [17-19]. Previous studies of serial OCT examinations have reported that most edge dissections have resolved at the 6–8-month follow-up [15,16]. Furthermore, a previous OCT study demonstrated that non–flow-limiting stent edge dissections, which had shorter longitudinal extension, and were superficial, with their depths limited to the intimal / atheroma layer detected by OCT, was not associated with increased short- and

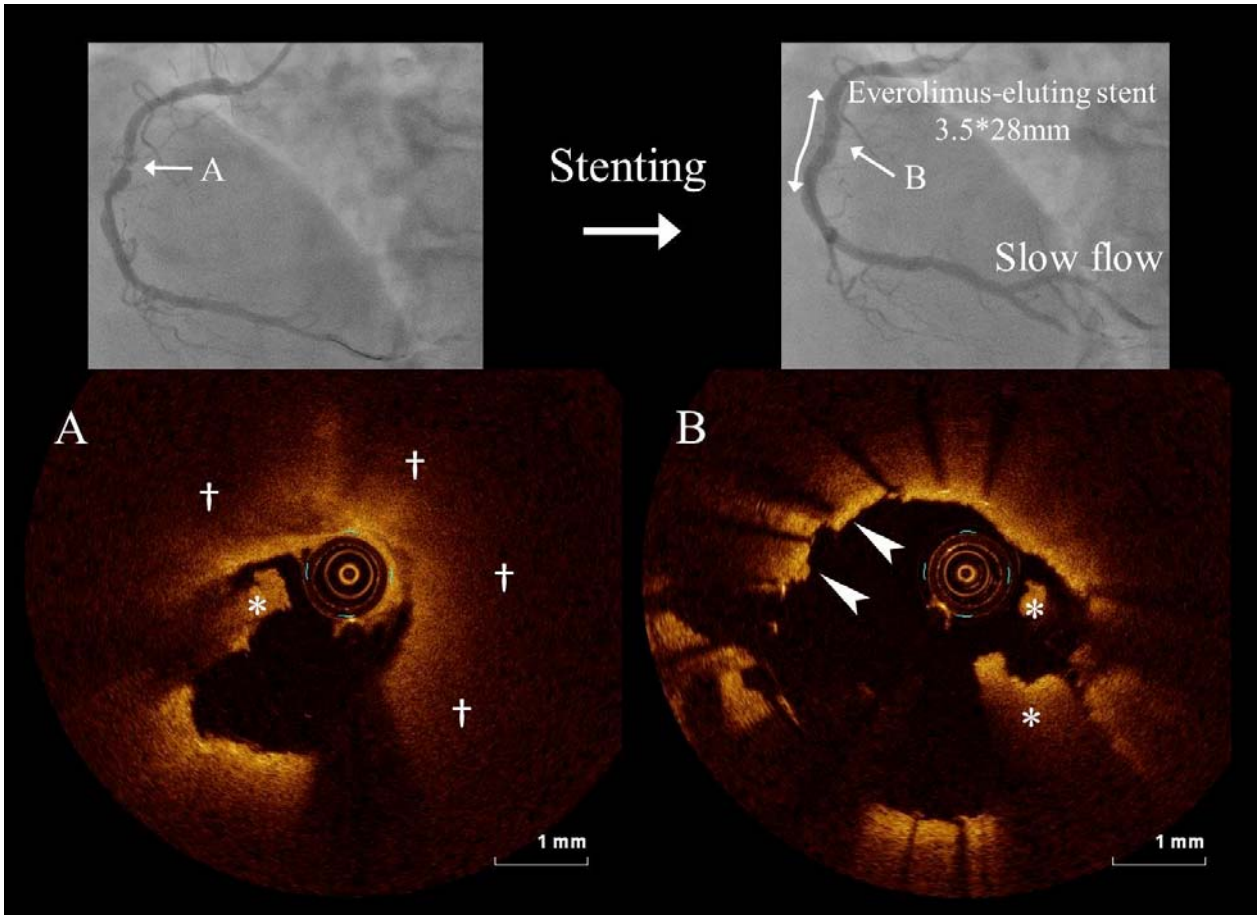

Figure 2: Relationship between intracoronary thrombus and tissue protrusion after stenting.

PCI was performed for the treatment of a mid-right coronary artery lesion in a patient with non-ST-elevation myocardial infarction. Cross-sectional OCT image at pre-intervention contains thrombus (dagger) and lipidic plaque (asterisks) (**A**). Angiography after stenting shows slow flow (left panel), and OCT disclosed a high-grade tissue protrusion between the stent struts (**B**). OCT, optical coherence tomography; PCI, percutaneous coronary intervention.

mid-term incidence of major adverse cardiac event (MACE) including stent thrombosis [18]. In case of stent edge dissection without narrowing of the true lumen, no additional procedure such as another stenting may be required for the treatment of dissection. Thus, OCT is a useful imaging device for predicting the occurrence of stent edge dissection and deciding the treatment strategy of it during PCI.

Incomplete Stent Strut Apposition

OCT has a limited ability to visualize through the optically opaque stent struts. The stent surface is located at the center of the stent strut blooming. Acute incomplete stent strut apposition (ISA) (Figure **1D**) is defined as the measured distance from the stent surface to the lumen contour being greater than the total thickness of the stent strut and polymer [14-16, 19, 20]. Acute ISA is commonly observed immediately after stenting. The incidence of it varies from 10 to 60% according to underlying plaque characteristics, especially, in calcified lesions responsible for nonuniform stent expansion [4, 16, 21, 22]. OCT-detectable minor acute ISA that is below the resolution of IVUS could be covered by neointima during 8-12 months follow-up. Previous OCT studies reported that 62-77% of acute ISA in the first-generation DESs and 74% in the second-generation DES resolved at 8-12 months follow-up [16, 22]. These studies have demonstrated that the best cut-off values of ISA distance at post-stenting for predicting late-persistent ISA at 8-12 months follow-up were > 260 -285 μm in the first generation DES and > 355 μm in the second generation DES, respectively. Thus, the second-generation everolimus-eluting stent (EES) could yield better healing of acute ISA in comparison with the first-generation DES. These data might help clinicians to avoid unnecessary additional procedures after stent implantation including high-pressure post-dilation with a larger diameter balloon. However, stent struts with a large persistent ISA may be an interruption of future PCI or a risk for stent thrombosis.

Calcium Fracture

Heavily calcified lesions in coronary arteries have been known as a contributing factor for stent underexpansion, which is associated with an increase in the risk of in-stent restenosis or stent thrombosis [23,24]. Kobayashi *et al*. demonstrated that the amount and extent of coronary calcification as assessed by OCT were associated with stent under-expansion and stent eccentricity [24]. Several studies have reported the effectiveness of plaque modification in heavily calcified lesions prior to stent implantation by using high pressure ballooning, cutting balloon angioplasty and rotational atherectomy [25-28]. OCT can visualize the plaque modification including calcium fracture during PCI (Figure **7**). More recently, Kubo *et al*. investigated clinical impact of coronary calcium fracture produced by PCI on the outcomes after EES implantation [29]. This study disclosed that the median calcium fracture thickness was 450μm (interquartile range 300 to 660μm), and lesions with calcium fracture acquired subsequent greater stent expansion (5.02 ± 1.43 mm2 vs. 4.33 ± 1.22 mm2, p = 0.047), resulting in lower frequency of binary restenosis (14% vs. 41%, p = 0.024) and target lesion revascularization (TLR) (7% vs. 28%, p = 0.046) at 10 months follow-up in comparison with those without. The presence of calcium fracture visualized by OCT imaging during PCI might be associated with favorable outcomes following PCI.

FOLLOW-UP EXAMINATIONS

Neointimal Coverage of the Stent

Long-term safety after DES implantation remains a clinical major concern due to persistent increase in the incidence of very late stent thrombosis (VLST) [30-33]. Among multiple risks of stent thrombosis [34], the extent of the stent coverage (ratio of uncovered struts to total struts) is the powerful predictor of for late stent thrombosis [35]. Compared to IVUS, OCT with its excellent resolution is capable of visualizing, quantifying thin neointimal hyperplasia after DES implantation, and distinguishing thin neointimal hyperplasia on stent struts and uncovered struts more reliably (Figure **3**) [36-38]. Previous validation studies have reported a good correlation of OCT imaging with histology for assessing the extent and thickness of neointimal coverage on stent struts [36, 39]. *In vivo* OCT study, Matsumoto *et al*. investigated 34 patients who underwent OCT examination at 6 months follow-up after sirolimus-eluting stent (SES) implantation [38]. Eighty-nine % of struts were covered by thin neointima. The median neointima thickness was 52.5 μm and 64% of neointima observed by OCT was undetectable by IVUS, which were less than 100 μm thickness. Chen *et al* demonstrated the delay in neointimal coverage after DES compared to bare-metal stent (BMS) [40]. The frequency of uncovered stent struts (17% vs. 0.3%, P<0.001) and malapposed stent struts (2% vs. 0%, P<0.001) was significantly higher in DES than in BMS at 8-month follow-up. Second-generation EES has been developed to improve the safety and efficacy of coronary stents by modifying the eluted drug, drug carrying system, polymer, and stent design [41,42]. The OCT sub-study of the randomized evaluation of sirolimus-eluting versus everolimus-eluting stent trial (RESET) showed more favorable vascular healing after second-generation EES compared to first-generation SES [43]. The frequency of uncovered stent struts [3 (0-17) % vs. 11 (2-34) %, p = 0.023], malapposed stent struts [0 (0-0) % vs. 0 (0-5) %, p = 0.006], and intra-stent thrombus (2% vs. 16%, P=0.022) was significantly lower in EES compared to SES at 9-month follow-up.

Several concerns have been raised regarding the long-term safety after DES implantation in patients with

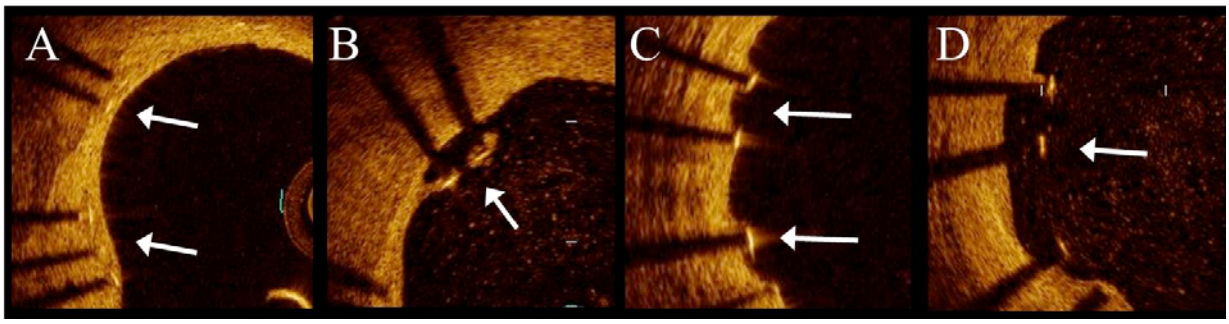

Figure 3: Each stent strut condition.

Each stent strut condition was classified as covered and apposed strut (**A**), covered and malapposed strut (**B**), uncovered and apposed strut (**C**), and uncovered and malapposed strut (**D**).

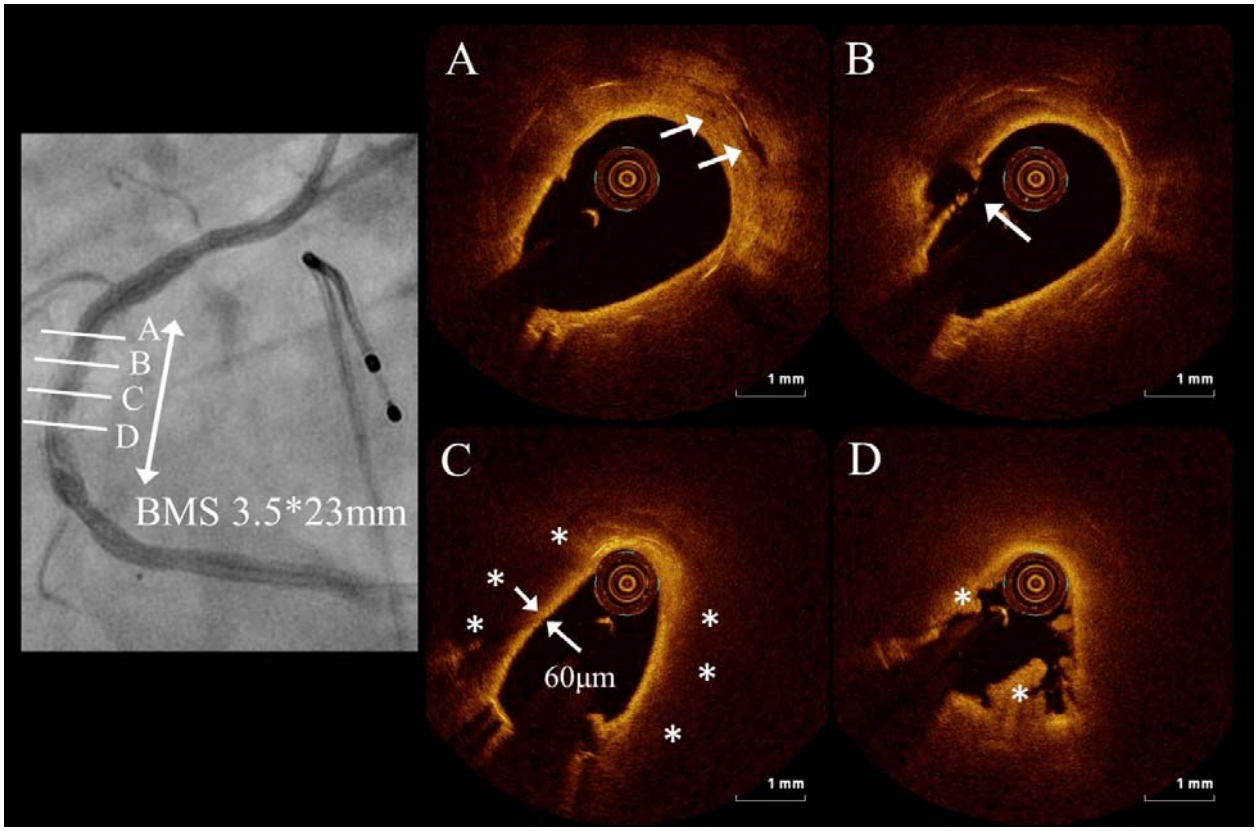

Figure 4: A case with neoatherosclerosis after bare metal stent implantation.

Angiography shows in-stent restenosis at 7 years after BMS implantation in the mid-right coronary artery. OCT visualizes micro vessel within neointima (arrow) (**A**), neointimal disruption (arrow) (**B**), lipid-laden neointima (dagger) (**C**) and thin-cap fibroatheroma-like neointima (cap thickness = 60 μm) (**C**), and thrombus (dagger) (**D**). BMS, bare metal stent.

acute coronary syndrome (ACS). Pathological studies reported that first-generation DES implantation in unstable coronary lesions might delay arterial healing and impair stent endothelialization [44, 45]. Because sirolimus and paclitaxel are highly lipophilic, it is likely that these agents have high affinity for lipid-rich plaques, dwell there for long periods of time, and influence healing by retarding smooth muscle cell proliferation and endothelial regrowth. In addition, lipid-rich necrotic cores have less vasculartur and fewer cells in plaques compared with fibrous dominant plaques. Kubo *et al*. disclosed the delayed healing process after first-generation SES in patients with unstable angina compared to stable angina. At 9-month follow-up, the frequency of lesion with malapposed stent strut (33% vs. 4%, P=0.012) and uncovered stent strut (72% vs. 37%, P=0.019) was significantly higher in the unstable angina group compared to stable angina [4]. The OCT sub-study of the HORIZONS-AMI trial showed that implantation of the first generation paclitaxel-eluting stent in acute MI significantly reduced neointimal hyperplasia, but resulted in higher rates of uncovered (5.7 ± 7.0 % vs. 1.1 ± 2.5 %, p < 0.001) and malapposed (0.9 ± 2.1 % vs. 0.1 ± 0.2 %, p < 0.001) stent struts at 13-month follow-up in comparison with BMS [46]. On the other hand, Ino *et al*. disclosed the safety and effectiveness of the second-generation EES in primary PCI for STEMI patients in OCT follow-up study [47]. At 10-month follow-up, there were no significant differences in the percentage of uncovered stent struts (1.6 ± 2.3 % vs. 1.2 ± 2.0 %, p=0.379) and malapposed stent struts (0.6 ± 1.2 % vs. 0.4 ± 0.9 %, p=0.596), and the frequency of intra-stent thrombus (13 % vs. 10 %, p=0.758) between EES and BMS. Sawada *et al*. also demonstrated the safety of the second-generation EES compared to the first-generation SES in patients with STEMI [48]. At 9-month follow-up, the frequency of the lesion with uncovered stent strut (72% vs. 37%, P=0.019) and malapposed stent strut (33% vs. 4%, P=0.012), and intra-stent thrombus (2.3% vs. 5.2%, P<0.001) was significantly higher in SES compared to EES. As above stated, neointimal coverage at the strut level assessed by OCT may be a surrogate marker for estimating the safety of DES according to the evidence concerning late stent thrombosis in the autopsy study [35]. In addition, the optimal duration of dual antiplatelet therapy after DES implantation has not been completely established. OCT

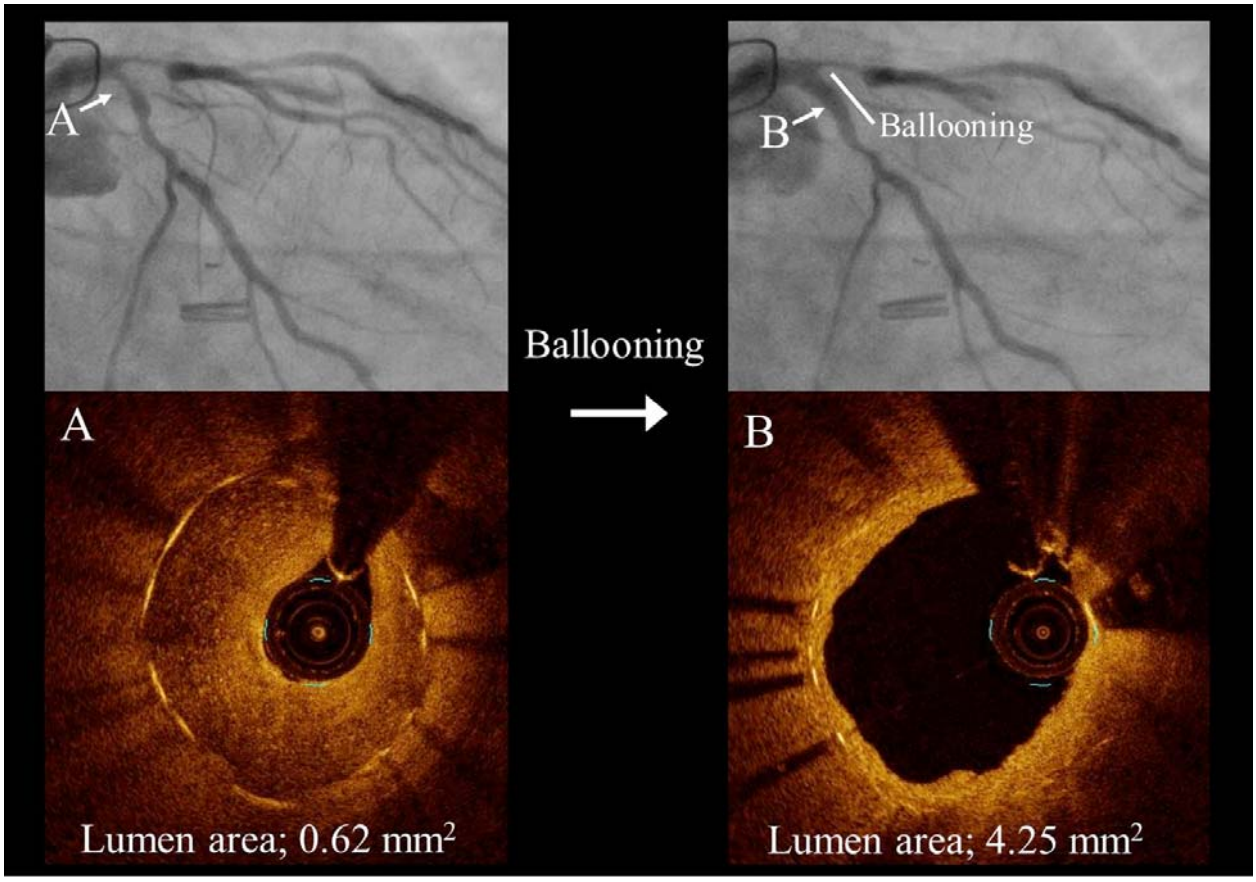

Figure 5: A case with in-stent restenosis after drug-eluting stent implantation.

Angiography shows in-stent restenosis at 9 months after EES implantation in the proximal-left circumflex artery (left panel). Cross-sectional OCT image at pre-intervention visualizes severe stenosis with heterogeneous tissue structure of neointima (**A**). Post ballooning angiography shows dilatation of in-stent restenosis lesion (right panel) and cross-sectional OCT image after ballooning visualizes increase of lumen area within in-stent restenosis lesion (**B**). EES, everolimus-eluting stent.

will provide important information about chronic DES status to determine the timing of the discontinuation of dual antiplatelet therapy.

Late Acquired Stent Malapposition

The role of acquired stent malapposition in the mechanism of late stent thrombosis remains controversial. A previous IVUS study demonstrated that stent malapposition was highly prevalent in patients with very late stent thrombosis after DES implantation [49]. A recent angiographic study reported that late acquired peri-stent contrast staining (PSS) after DES implantation might be caused by an abnormal vessel wall response such as stent malapposition and positive vessel remodeling, and was associated with very late stent thrombosis [50]. Furthermore, Tada *et al*. disclosed that the incidence of incomplete stent apposition (60.0% vs. 10%, P<0.001) and multiple interstrut hollows (85.0% vs. 25.7%, P<0.001), the frequency of uncovered stent struts (11.6 ± 10.0 % vs. 3.9± 6.0 %, P=0.001), malapposed stent struts (2.0% ± 7.0 % vs. 0.0 ± 0.0 %, P<0.001), and thrombus (35% vs. 10%, P=0.012) assessed by OCT were frequently observed in lesions with PSS than in lesions without PSS [51]. These results suggested that PSS was associated with endothelial delayed healing and could be a risk factor for stent thrombosis. Guagliumi *et al*. investigated the underlying mechanisms of late stent thrombosis after DES implantation in an explorative study with OCT and IVUS [52]. In their in-vivo case–control study, malapposed struts as assessed by OCT (the frequency of malapposed struts/ patient; 4.60 [1.85–7.19] % vs. 1.81 [0.00–2.99] %, P=0.001) and positive remodeling as assessed by IVUS (mean vessel cross-sectional area; 19.4±5.8 mm^2 vs. 15.1±4.6 mm^2, P=0.003) were associated with late stent thrombosis. These results supported prior autopsy studies suggesting the association of delayed healing, lack of endothelial cell coverage, and/or vascular toxicity with late stent thrombosis after DES implantation. OCT may provide important insight into

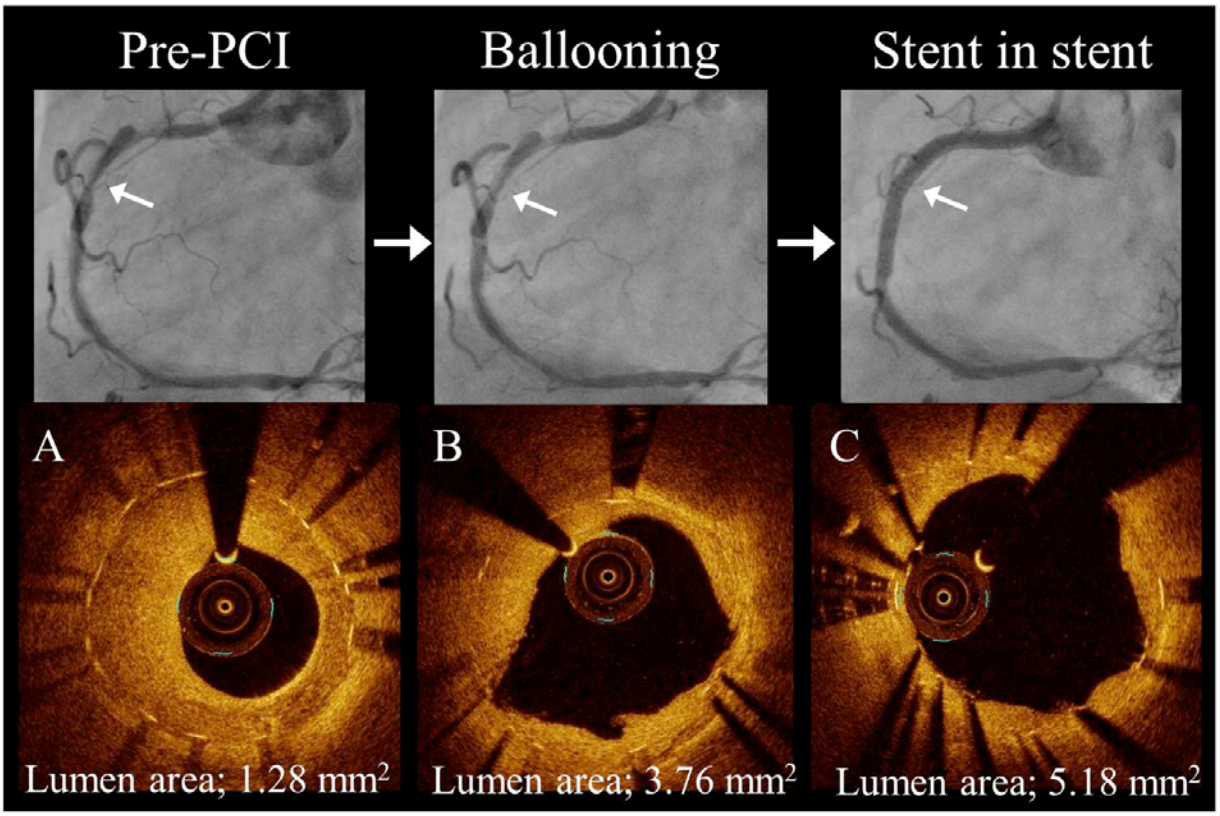

Figure 6: A case with in-stent restenosis after bare metal stent implantation.

Angiography shows in-stent restenosis at 6 months after BMS implantation in the proximal- right coronary artery (left panel). Cross-sectional OCT image at pre-intervention visualizes severe stenosis with homogeneous tissue structure of neointima (**A**). Cross-sectional OCT image after cutting balloon dilatation visualizes increase of lumen area within in-stent restenosis lesion (**B**). Cross-sectional OCT image after drug-eluting stent implantation visualizes further increase of lumen area (**C**).

the underlying mechanisms of late stent thrombosis after DES implantation (Figure **8**).

In-Stent Restenosis

In-stent restenosis (ISR) is an important unresolved issue even in the DES era, and its mechanism is not fully understood [53,54]. Several pathologic studies demonstrated that neointimal tissue (NIT) after stent implantation has various components including proteoglycans, organized thrombi, smooth muscle cells, atheromas, inflammatory cells, and fibrinoids [35, 55-57]. OCT is a useful imaging modality for evaluating not only the extent and amount of neointima but also the tissue characteristics of neointimal hyperplasia *in vivo* [58-60]. With respect to tissue characteristics, Gonzalo *et al* propounded a classification of the OCT appearance of restenotic tissue as the following 3 types, homogeneous, heterogeneous, or layered type [58]. The homogeneous appearance is commonly observed in restenosis of BMS, which is composed of smooth muscle cells with regeneration of dense collagen fibers (Figure **6**) [61]. On the other hand, a heterogeneous or layered appearance is often observed in restenosis of DES, which includes mature/immature smooth muscle cells and persistent fibrin or extracellular matrix, such as proteoglycans (Figure **5**) [62]. Nagoshi *et al*. demonstrated that the morphologic OCT patterns of the NIT in ISR differed between DES and BMS [60]. In the DES group, a layered pattern was seen in 53.2% of ISR lesions, whereas in the BMS group, a homogeneous pattern was seen in 76.7% of ISR lesions. The reduction in NIT area after balloon angioplasty was significantly smaller in lesions with the homogeneous pattern than in those with the layered or heterogeneous pattern (reduction rate: homogeneous 29.5±11.9% vs. layered: 42.2±15.7% vs. heterogeneous: 46.3±12.9%; P<0.01). Tada *et al*. investigated the impact of the morphologic OCT patterns of the NIT in ISR lesion on mid-term results (6–8 months) after paclitaxel-coated balloon (PCB) dilatation compared with plain old balloon angioplasty (POBA) [63]. This study demonstrated that both ISR and TLR rates of lesions with a homogeneous structure were significantly lower in the PCB group than those in the POBA group (ISR: 20.0 % vs. 55.6%, P =

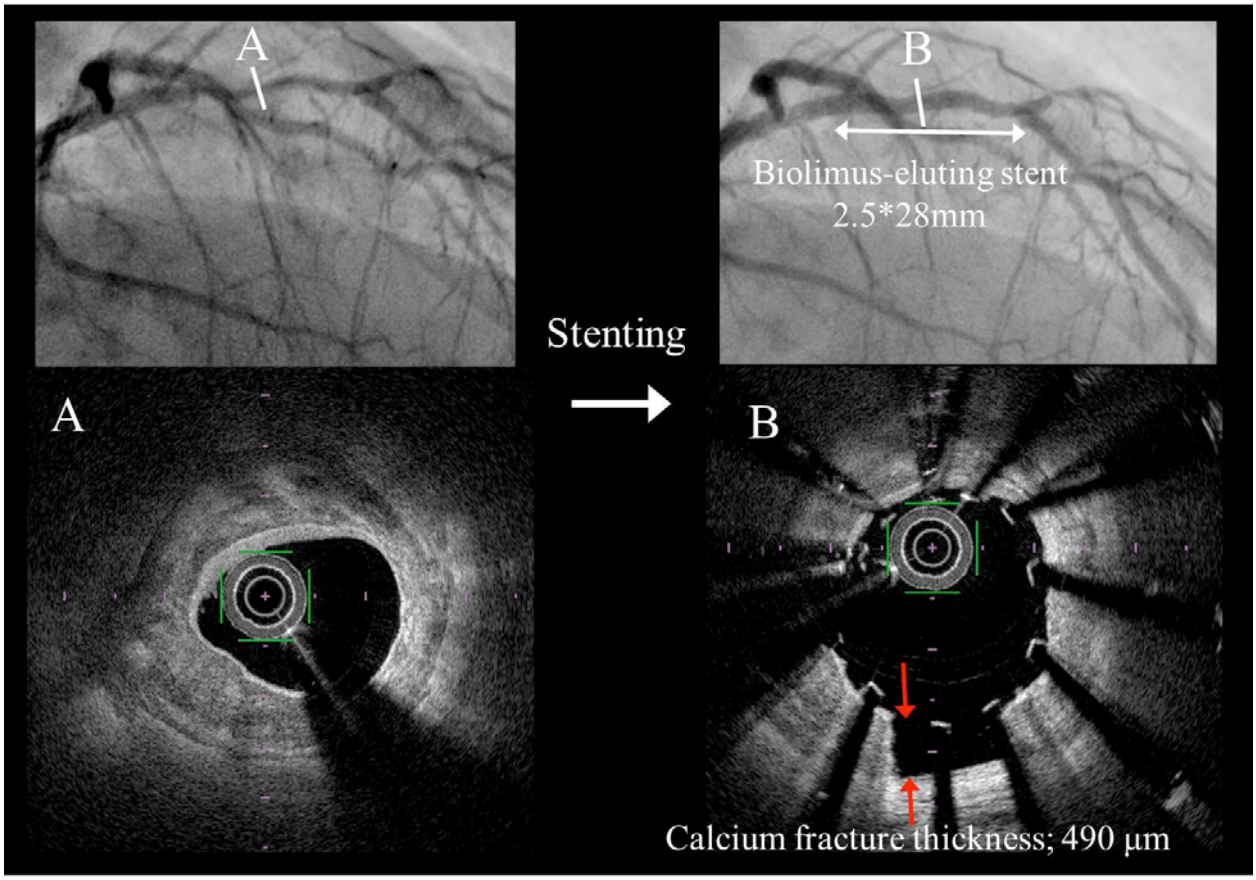

Figure 7: A case with severe calcified lesion.

Angiography shows severe stenosis with severe calcification in the proximal left anterior descending artery (left panel). Cross-sectional OCT image at pre-intervention visualizes entire circumferential calcium (**A**). Cross-sectional OCT image after drug-eluting stent implantation visualizes calcium fracture (6 o'clock). Thickness of the calcium fracture was 490 μm (red arrows) (**B**).

0.002, TLR: 12.7% vs. 37.0%, P = 0.019), but there was no difference between the two groups in ISR and TLR rates of lesions with a heterogeneous or layered structure. Both ISR and TLR rates of lesions with high backscatter were significantly lower in the PCB group than those in the POBA group (ISR: 19.8% vs. 52.5%, P < 0.001, TLR: 13.6 % vs. 42.5%, P = 0.001), but there was no difference between the two groups in ISR and TLR rates of lesions with low backscatter (ISR: 27.7% vs. 35.7%, P = 0.467, TLR: 23.1 % vs. 28.6%, P = 0.606). Morphological OCT evaluation of restenosis tissue may offer important clinical information about treatment strategies for ISR lesion and the acute/mid-term clinical outcome. Furthermore, validation study of the *in vivo* OCT findings in comparison with histology may allow us to understand the pathophysiology of ISR.

Neoatherosclerosis

Although it is generally recognized that the long-term clinical outcome of bare-metal stent (BMS) is favorable, the late luminal narrowing with restenosis of BMS can occur during extended follow-up (beyond 4 years), resulting in clinical events such as stent thrombosis and MI [64]. Pathological and OCT studies have disclosed that atherosclerotic change could develop over time in the neointimal tissue within the BMS, which has been termed "neoatherosclerosis" [65-69]. Inoue *et al*. have reported that stainless steel stents evoke a remarkable foreign body inflammatory reaction to the metal and persistent peri-strut chronic inflammatory cells may accelerate new atherosclerotic changes and consequent plaque vulnerability of the neointimal tissue around the stent struts [65]. Hasegawa *et al*. showed that new atherosclerotic progression occurred in neointima within BMS by using *in vivo* atherectomy specimens [66]. Takano *et al*. showed by using OCT that lipid-laden neointima (13.6 % vs. 42.5%, P<0.001), which was characterized by marked signal attenuation and a diffuse border, intimal disruption (38% vs. 0%, p < 0.001), and thrombus (52% vs. 5%, p < 0.01), were more frequently detected

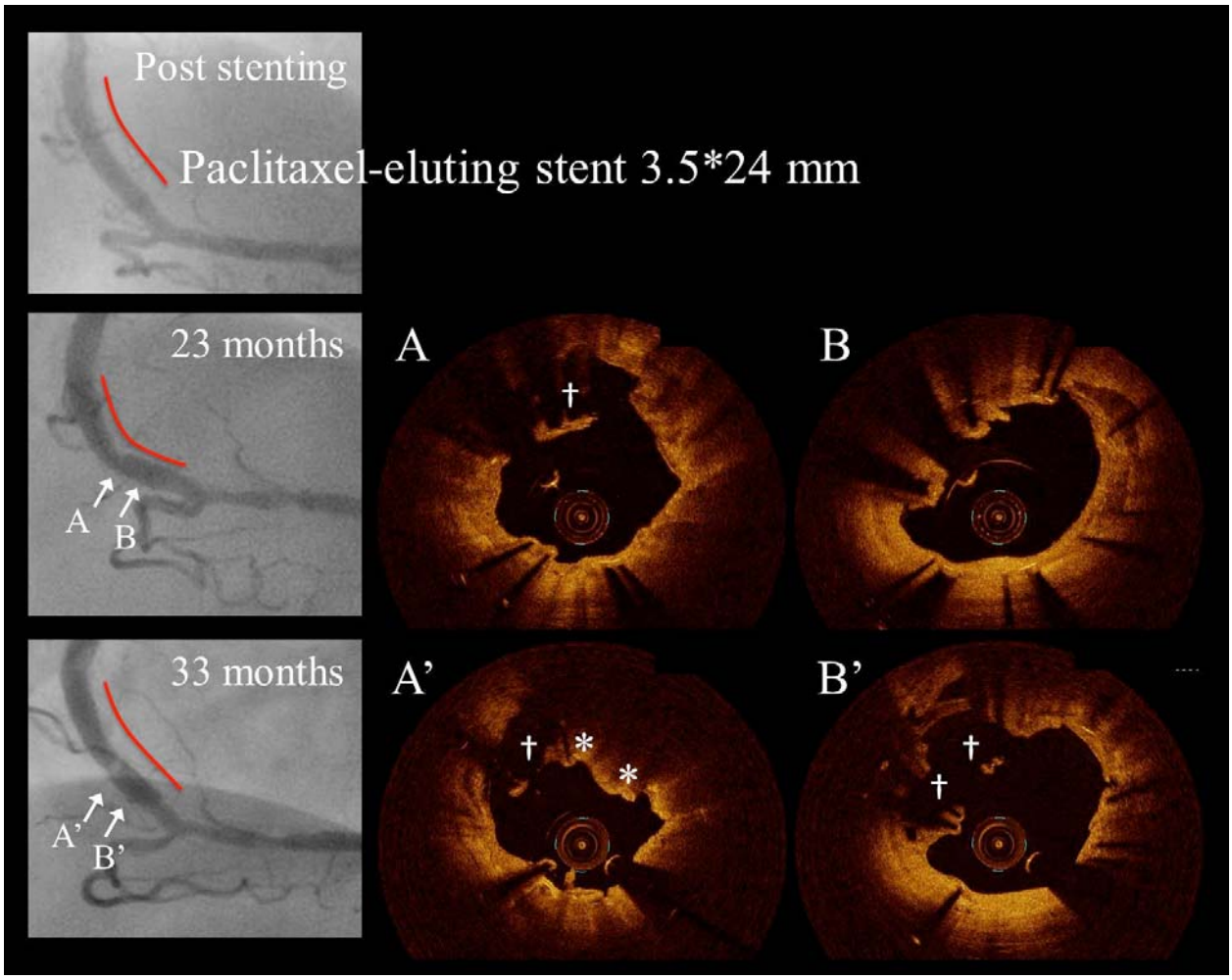

Figure 8: A case with late acquired stent malapposition.

Cross-sectional OCT images at 23 months after PES implantation show late acquired stent malapposition (asterisk) (**A**). Cross-sectional OCT images at 33 months after PES implantation show intra-stent thrombus (daggers) (**A'**) at the late acquired stent malapposition site and new late acquired stent malapposition (asterisks) (**B'**). PES, paclitaxel-eluting stent.

late (>5 years) compared to early (<6 months) after BMS implantation [68]. Furthermore, the appearance of intraintima neovascularization was more prevalent in the late phase than the early phase (62% vs. 0%, p < 0.01). The result suggested that expansion of neovascularization from peri-stent to intra-intima may contribute to atherosclerotic progression of neointima. In-stent neoatherosclerosis could occur earlier after DES implantation than after BMS implantation. Pathological study by Nakazawa *et al*. reported that atherosclerotic change within the neointima after BMS implantation did not begin to appear until 2 years and remained a rare finding until 4 years, whereas that after DES implantation was seen in about 60% of cases by 18 months [67, 69]. Kang *et al*. demonstrated that the first generation DES ≥20 months in comparison with DES <20 months after implantation had a higher incidence of TCFA-containing neointima (69% versus 33%, P = 0.012) and red thrombi (27% versus 0%, P = 0.007) assessed by OCT [70]. Ino *et al*. also demonstrated that late ISR lesion of SES (>1 year after implantation) in comparison with early ISR lesion of SES (<1 year) had a higher incidence of micro-channels within neointima (67% vs. 27%, p=0.007) and neointimal disruption (33% vs. 3%, p=0.008) [59]. Lee *et al*. also showed that neoatherosclerosis was less common in ISR lesions treated with the second-generation DES compared to the first-generation DES (10.8% vs. 45.5%, P<0.001), whereas the stent age of ISR lesions treated with the second-generation DES compared to the first-generation DES was significantly shorter [12.4 (10.6–21.1) months vs. 55.4 (34.4–80.4) months, P<0.001] [71]. The clinical presentation of neoatherosclerosis was significantly associated with the onset of acute coronary syndrome or stent thrombosis at follow-up (19.0% vs. 3.9%, P=0.001) (Figure **4**). The efficacy of PCI for the ISR lesions with neoatherosclerosis is controversial because peri-

procedural MI is significantly associated with the amount and characteristics of atherosclerotic plaque [72]. A previous study using OCT and near-infrared spectroscopy reported that neoatherosclerosis was associated with significantly reduced minimal cap thickness and nearly half of patients with periprocedural MI had neoatherosclerosis at the culprit site [73]. A recent study demonstrated that the incidence of post-PCI CK-MB elevation was higher in patients with neoatherosclerosis than in those without neoatherosclerosis (34.2% vs. 8.0%, p<0.001), and the maximum length of segments with neoatherosclerosis [odds ratio (OR), 1.463; 95% confidence interval (CI), 1.090–1.962; p=0.011] and thin cap fibro atheroma (TCFA) (OR, 14.328; 95% CI, 1.118–183.628; p=0.041) were identified as independent predictors for post-PCI CK-MB elevation [74]. Neoatherosclerosis within both DES and BMS may be an important mechanism of very late stent failure, including stent thrombosis and restenosis. Furthermore, PCI for the ISR lesions with neoatherosclerosis concerns peri-procedural MI. Thus, OCT may provide important information about risk stratification in terms of PCI for ISR lesions with neoatherosclerosis.

LIMITATIONS

The current OCT system has several considerable limitations for the clinical applications. First, at the time of image acquisition, OCT requires vessel flushing for a blood-free imaging zone because the near-infrared light signals are attenuated by red blood cells. Therefore, the evaluation of left main trunk, ostial coronary lesions, severe stenotic lesions, or totally occluded lesions might be limited. Second, OCT has a relatively shallow axial penetration depth of 2 mm. The OCT signal does not reach the back wall of thick atherosclerotic lesions. The penetration depth of OCT depends on tissue characteristics of coronary plaques. OCT is not appropriate for the visualization of whole vessel and the evaluation of arterial remodeling and coronary aneurysm. The OCT system is particularly suitable for the assessment of the superficial plaque morphologies.

CONCLUSIONS

The development of OCT technology enables the precise evaluation of coronary microstructure and stent architecture. The high resolution imaging of OCT has provided new insights into vascular response immediately and late after stent implantation. This imaging technique will improve the clinical outcomes of patients undergoing PCI.

DISCLOSURE

None.

REFERENCES

[1] Yabushita H, Bouma BE, Houser SL, *et al*. Characterization of human atherosclerosis by optical coherence tomography. Circulation 2002; 106: 1640-1645. http://dx.doi.org/10.1161/01.CIR.0000029927.92825.F6

[2] Kubo T, Imanishi T, Takarada S, *et al*. Assessment of culprit lesion morphology in acute myocardial infarction: ability of optical coherence tomography compared with intravascular ultrasound and coronary angioscopy. J Am Coll Cardiol 2007; 50: 933-939. http://dx.doi.org/10.1016/j.jacc.2007.04.082

[3] Lowe HC, Narula J, Fujimoto JG, Jang IK. Intracoronary optical diagnostics current status, limitations, and potential. J Am Coll Cardiol Interv 2011; 4: 1257-1270. http://dx.doi.org/10.1016/j.jcin.2011.08.015

[4] Kubo T, Imanishi T, Takarada S, *et al*. Comparison of vascular response after sirolimus-eluting stent implantation between unstable angina pectoris and stable angina pectoris: a serial optical coherence tomography study. J Am Coll Cardiol Img 2008; 1: 475-484. http://dx.doi.org/10.1016/j.jcmg.2008.03.012

[5] Takano M, Yamamoto M, Mizuno M, *et al*. Late vascular responses from 2 to 4 years after implantation of sirolimus-eluting stents: serial observations by intracoronary optical coherence tomography. Circ Cardiovasc Interv 2010; 3: 476-483. http://dx.doi.org/10.1161/CIRCINTERVENTIONS.110.957118

[6] Takarada S, Imanishi T, Liu Y, *et al*. Advantage of next-generation frequency-domain optical coherence tomography compared with conventional time-domain system in the assessment of coronary lesion. Catheter Cardiovasc Interv 2010; 75: 202-206. http://dx.doi.org/10.1002/ccd.22273

[7] Okamura T, Gonzalo N, Gutiérrez-Chico JL, *et al*. Reproducibility of coronary Fourier domain optical coherence tomography: quantitative analysis of *in vivo* stented coronary arteries using three different software packages. EuroIntervention 2010; 6; 371-379. http://dx.doi.org/10.4244/EIJV6I1A62

[8] Ozaki Y, Kitabata H, Tsujioka H, *et al*. Comparison of contrast media and low-molecular-weight dextran for frequency-domain optical coherence tomography. Circ J 2012; 76: 922-927. http://dx.doi.org/10.1253/circj.CJ-11-1122

[9] Liu Y, Shimamura K, Kubo T, *et al*. Comparison of longitudinal geometric measurement in human coronary arteries between frequency-domain optical coherence tomography and intravascular ultrasound. Int J Cardiovasc Imaging 2014; 30: 271-277. http://dx.doi.org/10.1007/s10554-013-0330-7

[10] Orii M, Kubo T, Tanaka A, *et al*. Inter-scan reproducibility of geometric coronary artery measurements using frequency-domain optical coherence tomography. Int Heart J 2013; 54: 64-67. http://dx.doi.org/10.1536/ihj.54.64

[11] Satogami K, Ino Y, Kubo T, *et al*. Successful stenting with optical frequency domain imaging guidance for spontaneous coronary artery dissection. J Am Coll Cardiol Interv 2015; 8: e83-85. http://dx.doi.org/10.1016/j.jcin.2014.12.247

[12] Kubo T, Akasaka T, Shite J, *et al*. OCT compared with IVUS in a coronary lesion assessment: the OPUS-CLASS study. J Am Coll Cardiol Img 2013; 6: 1095-1104. http://dx.doi.org/10.1016/j.jcmg.2013.04.014

[13] Gonzalo N, Serruys PW, Okamura T, *et al*. Optical coherence tomography assessment of the acute effects of stent implantation on the native vessel wall: a systematic quantitative approach. Heart 2010; 95: 1913-1919. http://dx.doi.org/10.1136/hrt.2009.172072

[14] Choi SY, Witzenbichler B, Maehara A, *et al*. Intravascular ultrasound findings of early stent thrombosis after primary percutaneous intervention in acute myocardial infarction: a Harmonizing Outcomes with Revascularization and Stents in Acute Myocardial Infarction (HORIZONS-AMI) substudy. Circ Cardiovasc Interv 2011; 4: 239-247. http://dx.doi.org/10.1161/CIRCINTERVENTIONS.110.959791

[15] Kume T, Okura H, Miyamoto Y, *et al*. Natural history of stent edge dissection, tissue protrusion and incomplete stent apposition detectable only on optical coherence tomography after stent implantation. Circ J 2012; 76: 698-703. http://dx.doi.org/10.1253/circj.CJ-11-0845

[16] Kawamori H, Shite J, Shinke T, *et al*. Natural consequence of post-intervention stent malapposition, thrombus, tissue prolapse, and dissection assessed by optical coherence tomography at mid-term follow-up. Eur Heart J Cardiovasc Imaging 2013; 14: 865-875. http://dx.doi.org/10.1093/ehjci/jes299

[17] Gonzalo N, Serruys PW, Okamura T, *et al*. Relation between plaque type and dissections at the edges after stent implantation: An optical coherence tomography study. Int J Cardiol 2011; 150: 151-155. http://dx.doi.org/10.1016/j.ijcard.2010.03.006

[18] Chamié D, Bezerra HG, Attizzani GF, *et al*. Incidence, predictors, morphological characteristics, and clinical outcomes of stent edge dissections detected by optical coherence tomography. J Am Coll Cardiol Interv 2013; 6: 800-813. http://dx.doi.org/10.1016/j.jcin.2013.03.019

[19] Prati F, Di Vito L, Biondi-Zoccai G, *et al*. Angiography alone versus angiography plus optical coherence tomography to guide decision-making during percutaneous coronary intervention: the Centro per la Lotta contro l'Infarto-Optimisation of Percutaneous Coronary Intervention (CLI-OPCI) study. EuroIntervention 2012; 8: 823-829. http://dx.doi.org/10.1016/j.jcin.2013.03.019

[20] Bezerra HG, Costa MA, Guagliumi G, Rollins AM, Simon DI. Intracoronary optical coherence tomography: a comprehensive review clinical and research applications. J Am Coll Cardiol Interv 2009; 2: 1035-1046. http://dx.doi.org/10.1016/j.jcin.2009.06.019

[21] Bouma BE, Tearney GJ, Yabushita H, *et al*. Evaluation of intracoronary stenting by intravascular optical coherence tomography. Heart *20*03; 89: 317-320. http://dx.doi.org/10.1136/heart.89.3.317

[22] Shimamura K, Kubo T, Akasaka T, *et al*. Outcomes of everolimus-eluting stent incomplete stent apposition: a serial optical coherence tomography analysis. Eur Heart J Cardiovasc Imaging 2015; 16: 23-28. http://dx.doi.org/10.1093/ehjci/jeu174

[23] Fujimoto H, Nakamura M, Yokoi H. Impact of calcification on the long-term outcomes of sirolimus-eluting stent implantation: Subanalysis of the Cypher Post-Marketing Surveillance Registry. Circ J 2012; 76: 57-64. http://dx.doi.org/10.1253/circj.CJ-11-0738

[24] Kobayashi Y, Okura H, Kume T, *et al*. Impact of Target Lesion Coronary Calcification on Stent Expansion. Circ J 2014; 78: 2209-2214. http://dx.doi.org/10.1253/circj.CJ-14-0108

[25] Tanigawa J, Barlis P, Di Mario C. Heavily calcified coronary lesions preclude strut apposition despite high pressure balloon dilatation and rotational atherectomy: in-vivo demonstration with optical coherence tomography. Circ J 2008; 72: 157-160. http://dx.doi.org/10.1253/circj.72.157

[26] Vaquerizo B, Serra A, Miranda F, *et al*. Aggressive plaque modification with rotational atherectomy and/or cutting balloon before drug-eluting stent implantation for the treatment of calcified coronary lesions. J Interv Cardiol 2010; 23: 240-248. http://dx.doi.org/10.1111/j.1540-8183.2010.00547.x

[27] Furuichi S, Sangiorgi GM, Godino C, *et al*. Rotational atherectomy followed by drug-eluting stent implantation in calcified coronary lesions. EuroIntervention 2009; 5: 370-374. http://dx.doi.org/10.4244/V5I3A58

[28] Okura H, Hayase M, Shimodozono S, *et al* REDUCE Investigators. Restenosis Reduction by Cutting Balloon Evaluation. Mechanisms of acute lumen gain following cutting balloon angioplasty in calcified and noncalcified lesions: An Intravascular Ultrasound Study. Catheter Cardiovasc Interv 2002; 57: 429-436. http://dx.doi.org/10.1002/ccd.10344

[29] Kubo T, Shimamura K, Ino Y, *et al*. Superficial Calcium Fracture After PCI as Assessed by OCT. J Am Coll Cardiol Img 2015. pii: S1936-878X(15)00027-3.

[30] Daemen J, Wenaweser P, Tsuchida K, *et al*. Early and late coronary stent thrombosis of sirolimus-eluting and paclitaxel-eluting stents in routine clinical practice: data from a large two-institutional cohort study. Lancet 2007; 369: 667-678. http://dx.doi.org/10.1016/S0140-6736(07)60314-6

[31] Kastrati A, Mehilli J, Pache J, *et al*. Analysis of 14 trials comparing sirolimus-eluting stents with bare-metal stents. N Engl J Med 2007; 356: 1030-1039. http://dx.doi.org/10.1056/NEJMoa067484

[32] Wenaweser P, Daemen J, Zwahlen M, *et al*. Incidence and correlates of drug-eluting stent thrombosis in routine clinical practice. 4-year results from a large 2-institutional cohort study. J Am Coll Cardiol 2008; 52: 1134-1140. http://dx.doi.org/10.1016/j.jacc.2008.07.006

[33] Kimura T, Morimoto T, Nakagawa Y, *et al*. for the j-Cypher Registry Investigators. Antiplatelet therapy and stent thrombosis after sirolimus-eluting stent implantation. Circulation 2009; 119: 987-995. http://dx.doi.org/10.1161/CIRCULATIONAHA.108.808311

[34] Honda Y. Drug-eluting stents. Insights from invasive imaging technologies. Circ J 2009; 73: 1371-1380. Review. http://dx.doi.org/10.1253/circj.CJ-09-0377

[35] Finn AV, Joner M, Nakazawa G, *et al*. Pathological correlates of late drug-eluting stent thrombosis: strut coverage as a marker of endothelialization. Circulation 2007; 115: 2435-2441. http://dx.doi.org/10.1161/CIRCULATIONAHA.107.693739

[36] Suzuki Y, Ikeno F, Koizumi T, *et al*. *In vivo* comparison between optical coherence tomography and intravascular ultrasound for detecting small degrees of in-stent neointima after stent implantation. J Am Coll Cardiol Interv 2008; 1: 168-173. http://dx.doi.org/10.1016/j.jcin.2007.12.007

[37] Capodanno D, Prati F, Pawlowsky T, *et al*. Comparison of optical coherence tomography and intravascular ultrasound for the assessment of in-stent tissue coverage after stent implantation. EuroIntervention 2009; 5: 538-543. http://dx.doi.org/10.4244/EIJV5I5A88

[38] Matsumoto D, Shite J, Shinke T, *et al*. Neointimal coverage of sirolimus-eluting stents at 6-month follow-up: evaluated by optical coherence tomography. Eur Heart J 2007; 28: 961-967. http://dx.doi.org/10.1093/eurheartj/ehl413

[39] Murata A, Wallace-Bradley D, Tellez A, *et al*. Accuracy of optical coherence tomography in the evaluation of neointimal coverage after stent implantation. J Am Coll Cardiol Img 2010; 3: 76-84. http://dx.doi.org/10.1016/j.jcmg.2009.09.018

[40] Chen BX, Ma FY, Luo W, *et al*. Neointimal coverage of bare-metal and sirolimus-eluting stents evaluated with optical coherence tomography. Heart 2008; 94: 566-570. http://dx.doi.org/10.1136/hrt.2007.118679

[41] Kedhi E, Joesoef KS, McFadden E, *et al*. Second-generation everolimus-eluting and paclitaxel-eluting stents in real-life practice (COMPARE): a randomised trial. Lancet 2010; 375: 201-209. http://dx.doi.org/10.1016/S0140-6736(09)62127-9

[42] Sabate M, Cequier A, Iñiguez A, *et al*. Everolimus-eluting stent versus bare-metal stent in ST-segment elevation myocardial infarction (EXAMINATION): 1 year results of a randomised controlled trial. *Lancet* 2012; 380: 1482-1490. http://dx.doi.org/10.1016/S0140-6736(12)61223-9

[43] Kubo T, Akasaka T, Kozuma K, *et al*. RESET Investigators. Comparison of neointimal coverage between everolimus-eluting stents and sirolimus-eluting stents: an optical coherence tomography substudy of the RESET (Randomized Evaluation of Sirolimus-eluting versus Everolimus-eluting stent Trial). EuroIntervention 2015; 11: 564-571. http://dx.doi.org/10.4244/EIJV11I5A109

[44] Nakazawa G, Finn AV, Joner M, *et al*. Delayed arterial healing and increased late stent thrombosis at culprit sites after drug-eluting stent placement for acute myocardial infarction patients: an autopsy study. Circulation 2008; 118: 1138-1145. http://dx.doi.org/10.1161/CIRCULATIONAHA.107.762047

[45] Finn AV, Nakazawa G, Ladich E, Kolodgie FD, Virmani R. Does underlying plaque morphology play a role in vessel healing after drug eluting stent implantation? J Am Coll Cardiol Img 2008; 1: 485-488. http://dx.doi.org/10.1016/j.jcmg.2008.04.007

[46] Guagliumi G, Costa MA, Sirbu V, *et al*. Strut coverage and late malapposition with paclitaxel-eluting stents compared with bare metal stents in acute myocardial infarction: optical coherence tomography substudy of the Harmonizing Outcomes with Revascularization and Stents in Acute Myocardial Infarction (HORIZONS-AMI) Trial. Circulation 2011; 123: 274-281. http://dx.doi.org/10.1161/CIRCULATIONAHA.110.963181

[47] Ino Y, Kubo T, Tanaka A, *et al*. Comparison of vascular response between everolimus-eluting stent and bare metal stent implantation in ST-segment elevation myocardial infarction assessed by optical coherence tomography. Eur Heart J Cardiovasc Imaging 2015; 16: 513-520. http://dx.doi.org/10.1093/ehjci/jeu227

[48] Sawada T, Shinke T, Otake H, *et al*. Comparisons of detailed arterial healing response at seven months following implantation of an everolimus- or sirolimus-eluting stent in patients with ST-segment elevation myocardial infarction. Int J Cardiol 2013; 168: 960-966. http://dx.doi.org/10.1016/j.ijcard.2012.10.043

[49] Cook S, Wenaweser P, Togni M, *et al*. Incomplete stent apposition and very late stent thrombosis after drug-eluting stent implantation. Circulation 2007; 115: 2426-2434. http://dx.doi.org/10.1161/CIRCULATIONAHA.106.658237

[50] Imai M, Kadota K, Goto T, *et al*. Incidence, risk factors, and clinical sequelae of angiographic peri-stent contrast staining after sirolimus-eluting stent implantation. Circulation 2011; 123: 2382-2391. http://dx.doi.org/10.1161/CIRCULATIONAHA.110.003459

[51] Tada T, Kadota K, Hosogi S, *et al*. Optical coherence tomography findings in lesions after sirolimus-eluting stent implantation with peri-stent contrast staining. Circ Cardiovasc Interv 2012; 5: 649-656. http://dx.doi.org/10.1161/CIRCINTERVENTIONS.112.968487

[52] Guagliumi G, Sirbu V, Musumeci G, *et al*. Examination of the *in vivo* mechanisms of late drug-eluting stent thrombosis: findings from optical coherence tomography and intravascular ultrasound imaging. JACC Cardiovasc Interv 2012; 5: 12-20. http://dx.doi.org/10.1016/j.jcin.2011.09.018

[53] Dangas GD, Claessen BE, Caixeta A, Sanidas EA, Mintz GS, Mehran R. In-stent restenosis in the drug-eluting stent era. Review. J Am Coll Cardiol 2010; 56: 1897-1907. http://dx.doi.org/10.1016/j.jacc.2010.07.028

[54] Ino Y, Kubo T, Kitabata H, *et al*. Impact of hinge motion on in-stent restenosis after sirolimus-eluting stent implantation. Circ J 2011; 75: 1878-1884. http://dx.doi.org/10.1253/circj.CJ-10-1182

[55] Schwartz RS, Chronos NA, Virmani R. Preclinical restenosis models and drug-eluting stents: Still important, still much to learn. J Am Coll Cardiol 2004; 44: 1373-1385. http://dx.doi.org/10.1016/j.jacc.2004.04.060

[56] Joner M, Finn AV, Farb A, *et al*. Pathology of drug-eluting stents in humans: delayed healing and late thrombotic risk. J Am Coll Cardiol 2006; 48: 193-202. http://dx.doi.org/10.1016/j.jacc.2006.03.042

[57] Hao H, Ishibashi-Ueda H, Tsujimoto M, *et al*. Drug-eluting stent: importance of clinico-pathological correlations. Circ J 2011; 75: 1548-1558. http://dx.doi.org/10.1253/circj.CJ-11-0393

[58] Gonzalo N, Serruys PW, Okamura T, *et al*. Optical coherence tomography patterns of stent restenosis. Am Heart J 2009; 158: 284-293. http://dx.doi.org/10.1016/j.ahj.2009.06.004

[59] Ino Y, Kubo T, Kitabata H, *et al*. Difference in neointimal appearance between early and late restenosis after sirolimus-eluting stent implantation assessed by optical coherence tomography. Coron Artery Dis 2013; 24: 95-101. http://dx.doi.org/10.1097/MCA.0b013e32835c872b

[60] Nagoshi R, Shinke T, Otake H, *et al*. Qualitative and quantitative assessment of stent restenosis by optical coherence tomography: comparison between drug-eluting and bare-metal stents. Circ J 2013; 77: 652-660. http://dx.doi.org/10.1253/circj.CJ-12-0610

[61] Kume T, Akasaka T, Kawamoto T, *et al*. Visualization of neointima formation by optical coherence tomography. Int Heart J 2005; 46: 1133-1136. http://dx.doi.org/10.1536/ihj.46.1133

[62] Nagai H, Ishibashi-Ueda H, Fujii K. Histology of highly echolucent regions in optical coherence tomography images from two patients with sirolimus-eluting stent restenosis. Catheter Cardiovasc Interv 2010; 75: 961-963. http://dx.doi.org/10.1002/ccd.22267

[63] Tada T, Kadota K, Hosogi S, *et al*. Association between tissue characteristics evaluated with optical coherence tomography and mid-term results after paclitaxel-coated balloon dilatation for in-stent restenosis lesions: a comparison with plain old balloon angioplasty. Eur Heart J Cardiovasc Imaging 2014; 15: 307-315. http://dx.doi.org/10.1093/ehjci/jet165

[64] Doyle B, Rihal CS, O'Sullivan CJ, *et al*. Outcomes of stent thrombosis and restenosis during extended follow-up of patients treated with bare-metal coronary stents. Circulation 2007; 116: 2391-2398. http://dx.doi.org/10.1161/CIRCULATIONAHA.107.707331

[65] Inoue K, Abe K, Ando K, *et al*. Pathological analyses of long-term intracoronary Palmaz-Schatz stenting. Is its efficacy permanent? Cardiovasc Pathol 2004; 13: 109-115. http://dx.doi.org/10.1016/S1054-8807(03)00132-7

[66] Hasegawa K, Tamai H, Kyo E, *et al*. Histopathological findings of new in-stent lesions developed beyond five years. Catheter Cardiovasc Interv 2006; 68: 554-558. http://dx.doi.org/10.1002/ccd.20787

[67] Nakazawa G, Otsuka F, Nakano M, *et al*. The pathology of neoatherosclerosis in human coronary implants bare-metal

and drug-eluting stents. J Am Coll Cardiol 2011; 57: 1314-1322.
http://dx.doi.org/10.1016/j.jacc.2011.01.011

[68] Takano M, Yamamoto M, Inami S, *et al*. Appearance of lipid-laden intima and neovascularization after implantation of bare metal stents: extended late phase observation by intracoronary optical coherence tomography. J Am Coll Cardiol 2009; 55, 26-32.
http://dx.doi.org/10.1016/j.jacc.2009.08.032

[69] Park SJ, Kang SJ, Virmani R, Nakano M, Ueda Y. In-stent neoatherosclerosis: a final common pathway of late stent failure. J Am Coll Cardiol 2012; 59: 2051-2057.
http://dx.doi.org/10.1016/j.jacc.2011.10.909

[70] Kang SJ, Mintz GS, Akasaka T, *et al*. Optical coherence tomographic analysis of in-stent neoatherosclerosis after drug-eluting stent implantation. Circulation 2011; 123: 2954-2963.
http://dx.doi.org/10.1161/CIRCULATIONAHA.110.988436

[71] Lee SY, Hur SH, Lee SG, *et al*. Optical coherence tomographic observation of in-stent neoatherosclerosis in lesions with more than 50% neointimal area stenosis after second-generation drug-eluting stent implantation. Circ Cardiovasc Interv 2015; 8: e001878.
http://dx.doi.org/10.1161/CIRCINTERVENTIONS.114.001878

[72] Lee T, Yonetsu T, Koura K, *et al*. Impact of coronary plaque morphology assessed by optical coherence tomography on cardiac troponin elevation in patients with elective stent implantation. Circ Cardiovasc Interv 2011; 4: 378-386.
http://dx.doi.org/10.1161/CIRCINTERVENTIONS.111.962506

[73] Ali ZA, Roleder T, Narula J, *et al*. Increased thin-cap neoatheroma and periprocedural myocardial infarction in drug-eluting stent restenosis: multimodality intravascular imaging of drug-eluting and bare-metal stents. Circ Cardiovasc Interv 2013; 6: 507-517.
http://dx.doi.org/10.1161/CIRCINTERVENTIONS.112.000248

[74] Lee SY, Hong MK, Shin DH, *et al*. Optical coherence tomography-based predictors for creatine kinase-myocardial band elevation after elective percutaneous coronary intervention for in-stent restenosis. Catheter Cardiovasc Interv 2015; 85: 564-572.
http://dx.doi.org/10.1002/ccd.25643

Received on 19-02-2016 Accepted on 05-04-2016 Published on 14-05-2016

DOI: http://dx.doi.org/10.12970/2311-052X.2016.04.01.5